Thin Solid Films 517 (2009) 5728–5733

Contents lists available at ScienceDirect

Thin Solid Films

journal homepage: www.elsevier.com/locate/tsf

Rapid thermal annealing and conventional furnace effect on $SrBi_2Ta_2O_9$ thin films crystallization

Gerardo González-Aguilar [a,b,*], Isabel M. Miranda Salvado [b], M. Elisabete Costa [b]

[a] Unidade de Optoelectrónica, INESC-Porto, Rua do Campo Alegre 687, Porto 4169-007, Portugal
[b] Departamento de Engenharia Cerâmica e do Vidro, CICECO, Universidade de Aveiro, Campus de Santiago, Aveiro 3810-193, Portugal

ARTICLE INFO

Article history:
Received 7 January 2008
Received in revised form 23 February 2009
Accepted 26 February 2009
Available online 9 March 2009

Keywords:
Ferroelectrics
Kinetics
Thermodynamics
Sintering
Arrhenius

ABSTRACT

The effect of rapid thermal annealing and conventional furnace annealing on the crystallization of $SrBi_2Ta_2O_9$ is modeled using an Arrhenius-type equation. Based on previous experimental results several authors have suspected that different reaction mechanisms occur depending of the heating rate employed in these two treatment methods. Oppositely, the results here presented and the analysis of reported data suggest two concurrent reaction mechanisms 1) direct transformation of the reagents into the perovskite phase and 2) transformation of an intermediate into the perovskite phase. Another important conclusion here obtained confirms the validity of the Arrhenius equation to predict the behavior of the crystallization process by either of the two heating methods mentioned above.

1. Introduction

$SrBi_2Ta_2O_9$ (SBT) is an extensively studied material for ferroelectric non-volatile random access memories applications [1–3]. Generally the preparation of SBT thin films by a chemical route requires the deposition of a precursor chemical solution on a selected substrate and its subsequent heat treatment until crystallization of the perovskite phase. Conventional Furnace Annealing (CFA) and Rapid Thermal Annealing (RTA) are amongst the most frequently used heating procedures. CFA consists on heating at low heating rates, typically less than 20 °C/min, in an electrical furnace, while RTA may be described as a heating treatment under heating rates exceeding 100 °C/s, usually using infrared radiation.

Several advantages of RTA for SBT thin film crystallization have been often reported: shorter processing times and better ferroelectric properties have been referred for RTA processed materials [2,4]. For the case of $Pb(Zr,Ti)O_3$ thin films which exhibit similar RTA benefits, Dang and Gooding [5,6] have proposed two related Landau Free-energy models to describe the perovskite formation reaction by RTA. While reproducing the experimental trends of perovskite formation by RTA [5,6], their models based on long-ranged interactions does not clarify the differences between the reactions under analysis, i.e. reagents-to-perovskite versus reagents-to-fluorite crystallization reactions. Moreover, no attempts were made to describe the CFA crystallization procedure with the proposed models.

It has been claimed that the properties improvement by RTA is the result of the thin film microstructure control achieved by this method [7]. However the exact way in which microstructure benefits the ferroelectrical properties remains obscure to date. Another issue to be clarified is why the very high heating rates employed in RTA processes should improve or speed-up the desired crystallization reactions while not affecting other (unwanted) reactions. The main purpose of this study is to develop a model that keeping the advantage of simplicity might explain the crystallization reaction processes occurring in both CFA and TFA annealing methods, with the objective of understanding the differences in the synthesis and properties of Aurivillius compound prepared by CFA and RTA.

2. Theoretical considerations

In the synthesis process of SBT at least three crystalline phases have been found. These are the fluorite, the perovskite and the pyrochlore phases. The first one has been considered to be an intermediate for the formation of the perovskite phase [8]. The pyrochlore phase has been observed in overheated samples and is attributed to bismuth volatilization. The present work will be focused on the transformations of the reactive phase leading to the fluorite and to the perovskite phase.

From thermodynamic and kinetic points of view, two possible situations may arise during the reaction of raw materials for producing SBT: 1) direct or 2) indirect transformation of the reagents into products. These situations imply three definite species with different potential energies, as illustrated in Fig. 1. The specie **A** is an unstable reactive complex, **B** is the fluorite phase and **C** is the perovskite phase.

* Corresponding author. Unidade de Optoelectrónica, INESC-Porto, Rua do Campo Alegre 687, Porto 4169-007, Portugal.
E-mail address: gaguilar@fc.up.pt (G. González-Aguilar).

0040-6090/$ – see front matter © 2009 Elsevier B.V. All rights reserved.
doi:10.1016/j.tsf.2009.02.143

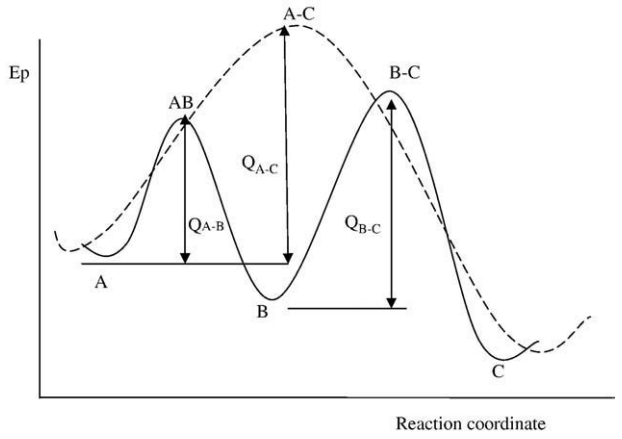

Fig. 1. Variation of Potential Energy (Ep) versus reaction coordinates for two possible mechanisms of SBT perovskite phase formation by CFA or RTA. Detailed explanations are offered in the text.

By the solid-line curve (Fig. 1) two processes of the indirect transformation (situation 1) are represented: **A→B** describing the reaction pathway from the reactive complex towards the fluorite phase and **B→C** applying to its consecutive transformation into the perovskite phase. Accordingly, the concentration of specie **B** will be decreased by the **B→C** subsequent process.

According to Kwak and Sung who studied the phase formation kinetics in SBT thin films using **CFA**, the reaction pathway **A→B→C** [8,9] was effectively probed. Moreover, the activation energy for SBT crystallization in thin films evolved from a fluorite phase previously obtained at 600 °C was calculated by these authors as being 264 kJ/mol. Whether the pathway **A→B→C** occurs when the samples are submitted to **RTA** has not been clarified yet. However, one may suspect it to occur, due to the worse electrical properties and morphology differences which distinguish the two step RTA treated films (a first RTA step at 550 °C followed by a second RTA step at 650 °C), from a single step treatment at 650 °C by RTA [10]. This point of view is further strengthened if the observed differences between CFA and RTA-one step heat treated thin films [3] are attributed to this mechanism.

The dashed-line curve **A→C** (Fig. 1) represents a direct pathway from the reactive complex to perovskite phase (situation 2), being the case when no fluorite phase is detected (for instance, single step RTA heat treated samples) [10,11]. Following the above reasoning, the observed differences between CFA and one step RTA heat treated thin films can be attributed to different reaction mechanisms.

Generally, the Arrhenius formalism can be used to describe the temperature dependence of any chemical reaction rate [12]. For a first order reaction X→Y, the rate of transformation of reagents into products (v_{X-Y}) is given by:

$$v_{X-Y} = -dC_X(t)/dt = dC_Y(t)/dt = k_{X-Y}{*}C_X(t) \quad (1)$$

where $C_Y(t)$ and $C_X(t)$ are the product and reagent concentration at time t and k_{X-Y} is the Arrhenius constant. k_{X-Y} may be expressed as:

$$k_{X-Y} = A_{X-Y}{*}e^{\frac{-Q_{X-Y}}{RT}} \quad (2)$$

where A_{X-Y} is a factor depending on the mechanism of the reaction X→Y, Q_{X-Y} is the activation energy of that reaction, which is equal to the energy gap between the state X and the activate complex X–Y, R is the gas constant and T is the absolute temperature.

Defining the conversion ratio of the specie X, r_X as:

$$r_X = \frac{[C_X(0) - C_X(t)]}{C_X(0)} \quad (3)$$

where $C_X(0)$ and $C_X(t)$ represent the reagent concentration at a time 0 and t, respectively. The r_X change rate is then:

$$\frac{dr_X}{dt} = -\frac{1}{C_X(0)}\frac{dC_X(t)}{dt} \quad (4)$$

Taking Eq. (1) into account, Eq. (4) can be expressed as

$$\frac{dr_X}{dt} = \frac{1}{C_X(0)}{*}k_{X-Y}{*}C_X(t)dt \quad (5)$$

Or, for a finite and small time variation and substituting Eq. (2)

$$\Delta r_{X-Y} = A_{X-Y}\frac{C_X(t)}{C_X(0)}{*}t{*}e^{\frac{-Q_{X-Y}}{RT}} \quad (6)$$

where Δr_{X-Y} is the conversion ratio relative to a given amount of the reactive complex (X) into the specific product (Y).

For a consecutive reaction scheme X→Y→Z one may define a net conversion of X (into Y), (here shortly called as NetΔr_{X-Y}) as:

$$\mathrm{Net}\Delta r_{X-Y} = \Delta r_{X-Y} - \Delta r_{Y-Z} \quad (7)$$

Δr_{Y-Z} may be calculated by applying Eq. (6) to the reaction Y→Z. Similarly for the coupled reaction scheme (X→Y→Z plus X→Z) one may define a net conversion of X (into Z) as

$$\mathrm{Net}\Delta r_{X-Z} = \Delta r_{X-Z} + \Delta r_{Y-Z} \quad (8)$$

in which Δr_{X-Z} and Δr_{Y-Z} are both calculated through equation (Eq. (6)).

The universal application of the Arrhenius classical formalism has been demonstrated by studies so widely different as the phase formation kinetics in SBT thin films obtained by CFA [8,9,13] or the grain growth kinetics in $CaTiO_3$:xFeO aggregates [14], it is noteworthy to state here that these studies were based in the assumption of a reaction described by a simple mechanism.

Some reported experimental facts [1,3,8,9,11,13–16] can help in the choice of some realistic starting assumptions to be used in modelling procedure here proposed:

1. The process **A→B** effectively occurs in CFA as the fluorite phase **B** is visible after short reaction times [8,9], though not reported until now in RTA. As mentioned before, the reported differences between single step and two step RTA crystallization support the assumption that the process **A→C** is predominant in single step RTA treated samples [3,11], whereas **A→B→C** may occur in a significant extent in the two step heated samples [8,9,11,13,14,17]. This does not exclude the simultaneous competing reaction **A→B→C** in a one step heated sample.
2. Based on the fact that the starting temperature of the formation of the fluorite phase **B** is lower than that respecting the formation of the perovskite phase **C** (600 °C versus 700 °C [8,9]) it is assumed that the activation energy of the process leading to the fluorite phase (Q_{A-B}) is lower than the activation energy needed for the formation of the perovskite phase Q_{A-C} or Q_{B-C} (for processes **A→C** or **B→C**, respectively).
3. As in RTA the crystallization of the perovskite phase **C** is completed at 650 °C (compare with 600 °C for fluorite formation in CFA) no fluorite (**B**) being left, it may be concluded that the A_{A-B} factor is lower than the A_{A-C} factor.
4. As the fluorite phase is observed when heat treatments are performed using low heating rates and during short times, the factor A_{B-C} is though not to exceed the A_{A-C} factor.

The above considerations allow to establish the necessary inputs for the comparative studies here described. The simulations that are going to be undertaken include:

i. The coupling of the reactions **A→B→C** and **A→C**. The interest of this coupling is to account for parallel reaction mechanisms in the

formation of the Aurivillius phase i.e. to not exclude the possibility of competing chemical mechanisms that can be favoured by the used heating rate. This coupling will be called the complex process.

ii. The coupling of the reactions **A→B** and **A→C**. In this case it is considered the formation of a sub-product that is unable to react. If existing, this mechanism only applies to RTA as in CFA the **B→C** reaction was observed [13]. This coupling will be called the simple process.

The Arrhenius equation was written into a C language program. The modelling procedure was time-driven, with time steps of 0.1 s. Following the experimental conditions currently reported, the heating rate was fixed as 100 °C/s for RTA simulations until a maximum temperature of 650 °C, followed by a dwell at 650 °C during the necessary time to complete the reaction, according to the usually reported experimental values [11]. For CFA simulations a heating rate of 5 °C/min was assumed until achieving a maximum temperature of 720 °C, followed by a dwell at 720 °C during the time required for completing the reaction [9,13].

The necessary data for pursuing the modelling were obtained from the literature, $Q_{B-C}=264$ kJ/mol [9,13], or settled as follows: Q_{A-C} is assumed to be nearly the same as Q_{B-C} in spite of the higher temperature of the **B→C** process and of its dependence on the **A→B** process to occur. Taking into consideration that the fluorite phase formation is completed at 650 °C in CFA experiments, which is 100 °C lower than the temperature of the complete crystallization of the perovskite phase, the value of Q_{A-B} was set to 164 kJ/mol. This was made in order to keep approximately constant the ratio Q/RT at the beginning of each reaction. This value somewhat arbitrary is used for a first cycle of calculations. The impact of such arbitrariness on the modelling results will be later accessed by varying the Q_{A-B} value.

The value of A_{A-C} was estimated by substituting in the kinetic equation (Eq. (6)) the activation energy ($Q=264$ kJ/mol) and temperature ($T=700$ °C) for a conversion rate of 50% ($r=0.5$ and $C_X(t)=0.5$), with values of $\Delta t=0.1$ s and $C_X(0)=1.0$. The A_{B-C} or A_{B-C} values were set to be 10 or 50 times smaller than A_{A-C} based on the considerations discussed previously. The values of the constants used and the nomenclature of the simulations are detailed in Table 1.

To avoid the problems of mathematical rounding, the model sets to 1 the probability of the reaction occurrence when the value of the ratio Q/RT is lower than 35. In other words, the reaction is allowed to start at a temperature which is 25 °C below the usual temperature used in all the experimental work here mentioned (see by instance [11] and [13]). This is a rational approximation, as this value is ~31 when $Q=264$ kJ/mol and $T=725$ °C (conditions for perovskite crystallization), or ~26 when $Q=164$ kJ/mol and $T=550$ °C (conditions for fluorite crystallization). The end of the reaction is assumed to be reached when the cumulative sum of the conversion ratios produced by all reactions is greater than 0.99 ($\sum_{i=1}^{n}\Delta r_i>0.99$) or the sum of the species formed in the last step plus the cumulative sum is greater than 1.0 ($\sum_{i=1}^{n}\Delta r_i+\Delta r_{n+1}>1.00$).

The samples CFA-Sn ($n=1,5$) are included for testing the suitability of the model mainly because the absence of the reaction **B→C** may contribute to a large increase of the final concentration of B contrarily to what is experimentally observed [8,9]. As the time spent by the system to evolve from 650 °C to 750 °C at the normal heating rates employed in CFA experiments (5–10 °C/min) is longer enough to guarantee the complete transformation of the reagents into the specie **B** before **A→C** becomes dominant, the necessary conditions for testing the model suitability are thus ensured.

3. Modelling results

In specific instances of the next discussion, both terms "conversion" and "concentration" will be used to refer the modelling results under analysis. The reason behind is that some results are better explained by using the concept of "conversion" while other results demand the concept "concentration" for purposes of comparing data with literature. The legitimacy for such equivalence of terms may be explained as follows: for two parallel reactions **X→Y** plus **X→Z**, with associated conversions r_{X-Y} and r_{X-Z}, the quotient of the final conversions is a normalized fractional amount ("concentration") of Y in Z:

$$C(Y)=\frac{\Delta r_{X-Y}}{\Delta r_{X-Z}}=\frac{Y(t)}{X(0)}*\frac{X(0)}{Z(t)}=\frac{Y(t)}{Z(t)}.$$

The results respecting the simulation of RTA are shown in Fig. 2. For the case of the simple process (RTA-S1,S5) the conversion of **A** into **B** increases linearly with the time, whereas in the case of the complex

Table 1
Nomenclature of the experiments and input data used in the modelling study.

Reaction schemes	Name	A	Q (kJ/mol)	Name	A	Q (kJ/mol)
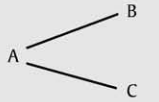 Simple process	RTA-S1	$A_{A-B}=10^{-4}$ $A_{A-C}=10^{-3}$	$Q_{A-B}=164$ $Q_{A-C}=264$	CFA-S1	$A_{A-B}=10^{-4}$ $A_{A-C}=10^{-3}$	$Q_{A-B}=164$ $Q_{A-C}=264$
	RTA-S5	$A_{A-B}=10^{-4}$ $A_{A-C}=5*10^{-3}$	$Q_{A-B}=164$ $Q_{A-C}=264$	CFA-S5	$A_{A-B}=10^{-4}$ $A_{A-C}=5*10^{-3}$	$Q_{A-B}=164$ $Q_{A-C}=264$
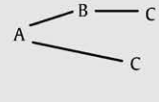 Complex process	RTA-X1	$A_{A-B}=10^{-4}$ $A_{B-C}=10^{-4}$ $A_{A-C}=10^{-3}$	$Q_{A-B}=164$ $Q_{B-C}=264$ $Q_{A-C}=264$	CFA-X1	$A_{A-B}=10^{-4}$ $A_{B-C}=10^{-4}$ $A_{A-B}=10^{-3}$	$Q_{A-B}=164$ $Q_{B-C}=264$ $Q_{A-C}=264$
	RTA-X5	$A_{A-B}=10^{-4}$ $A_{B-C}=10^{-4}$ $A_{A-C}=5*10^{-3}$	$Q_{A-B}=164$ $Q_{B-C}=264$ $Q_{A-C}=264$	CFA-X5	$A_{A-B}=10^{-4}$ $A_{B-C}=10^{-4}$ $A_{A-C}=5*10^{-3}$	$Q_{A-B}=164$ $Q_{B-C}=264$ $Q_{A-C}=264$

Note: X stands for complex process, S for simple process; RTA for Rapid Thermal Annealing and CFA for Conventional Thermal Annealing, the number after S or X represent the value of the constant A_{A-C}.

mechanism (**A→C** plus **A→B→C**) this tendency is no longer observed as the process **B→C** takes place. This last reaction originates **B** consumption which is reflected in a slowdown of the net conversion to **B**. It is observed that the conversion to **C** exhibits a very fast initial growth due to the conjugation of fast reaction kinetics with a fast temperature increase followed by a linear increase tendency.

It is noteworthy that in the case of a slow reaction rate (**A→C**) for the processes (RTA-S1 and RTA-X1), high degrees of **A** transformation into **B** are achieved for the simple process (**A→C** plus **A→B**) while for the complex mechanism (**A→C** plus **A→B→C**) the positive variation of the conversion of **A** into **B** runs in parallel to the conversion of **B** into **C**, despite their different activation energy values. Therefore the net conversion of **A** into **B** does not vanish. The different rates of both **B** production and **B** consumption processes are evidenced by the positive inflection of the Net Δr_{A-B} curve.

The comparison between RTA-S1,X1 and RTA-S5,X5 shows that in the second set of processes (RTA-S5 and RTA-X5) the conversion into **C** achieves a final value of 1 after 2×10^2 s which is 1/5 of the time required by the first set of processes (RTA-S1 and RTA-X1) for allowing equivalent values of conversion to be reached. This reflects the relation between their respective A_{A-C} values, i.e. $A_{A-C}(1) = 1/5\ A_{A-C}(5)$. In the RTA-S5 case the final value of the conversion of **A** into **B** and thereby of the final **B** fractional amount is approximately 2×10^{-2} whereas it is approximately 8×10^{-2} for RTA-S1, which is an amount detectable by X-ray Diffraction (XRD) analysis. This fact eliminates model RTA-S1 as an acceptable one, as no RTA experiments have reported the presence of a second phase; thus if second phases exist their concentration must be below the detection limit of the XRD analysis equipment which is generally around 5%. Though the elapsed time for the reagents to be converted into products in RTA-S1 is comparable with that experimentally reported [11], the equivalent time respecting RTA-S5 is too short to be accepted as a real one thus disqualifying this second model. These two arguments (reaction time and final value of fractional fluorite amount) seem to indicate that the description of the reaction by a simple mechanism (RTA-S1,S5) is not fully correct in none of the two RTA cases.

For the RTA-X5 and RTA-X1 (complex) processes the final values of the net conversion into **B** are very small ($\sim3\times10^{-4}$ and $\sim10^{-3}$ respectively), almost negligible, being thus compatible with the absence of second phases in the reviewed literature [11,18]. The reaction time corresponding to the RTA-X5 mechanism is too short when compared with the experimental ones [11]. Therefore the RTA-X1 mechanism seems to be the most suitable one for describing the rapid thermal annealing process.

The results describing the conventional furnace annealing (CFA) are presented in Fig. 3. The results after 30 min of reaction by the simple pathway (**A→B** plus **A→C**) reveal a very high final value of **B** concentration which has not been observed experimentally (0.18 for CFA-S5 and 0.20 for CFA-S1). However in the case of the complex pathways (**A→C** plus **A→B→C**) low quantities of fluorite remain at the end of the reaction (10% for CFA-X1 and 7% for CFA-X5, after 30 min of reaction). It is necessary to remind here than the criterion used to stop the calculations after 30 min was the fact that a new step would "transform" an amount of **B** superior to that existing effectively and thus physically unacceptable. In other words: our criterion to stop a reaction is purely mathematical and not physical; this is made in order to simplify the computational algorithm. The simulated reaction time (30 min) is in line with the time used by the present authors in the crystallization of SBT thin films [19,20], but not with the vast majority of the reported works. The longer experimental times usually reported (around 45–60 min) must decrease the calculated quantity of the secondary phase (fluorite) down to ~5%, in agreement with the results reported by several authors [8,9].

It can be concluded that fluorite is associated to a local minimum on the energetic surface of the reaction and that the activated system tends to this energy state through a slow structure relaxation (small A_{A-B} factor in the Arrhenius equation), despite the small activation energy. Once the system reaches this state, it is energetically unfavourable to continue the reaction. That is the cause of higher temperatures required by CFA treatment.

Contrarily, from the same initial state (activated complex **A**) it is possible to reach an energetically higher state, provided the supplied energy is high enough, leading the reaction to the global energetic minimum. This scenario has more importance in RTA treated samples.

In both RTA and CFA a complex (**A→C** plus **A→B→C**) pathway mechanism is possible and the final modelling results agree with the

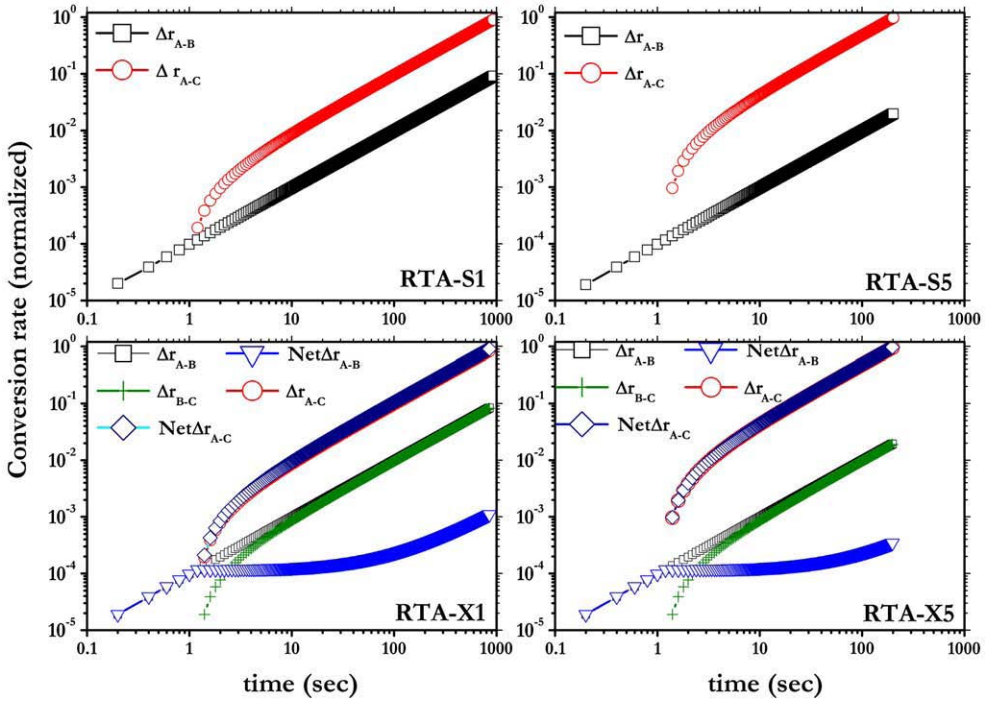

Fig. 2. Arrhenius simulation of a RTA processing: upper graphs stand for the simple model and bottom graphs for the complex model.

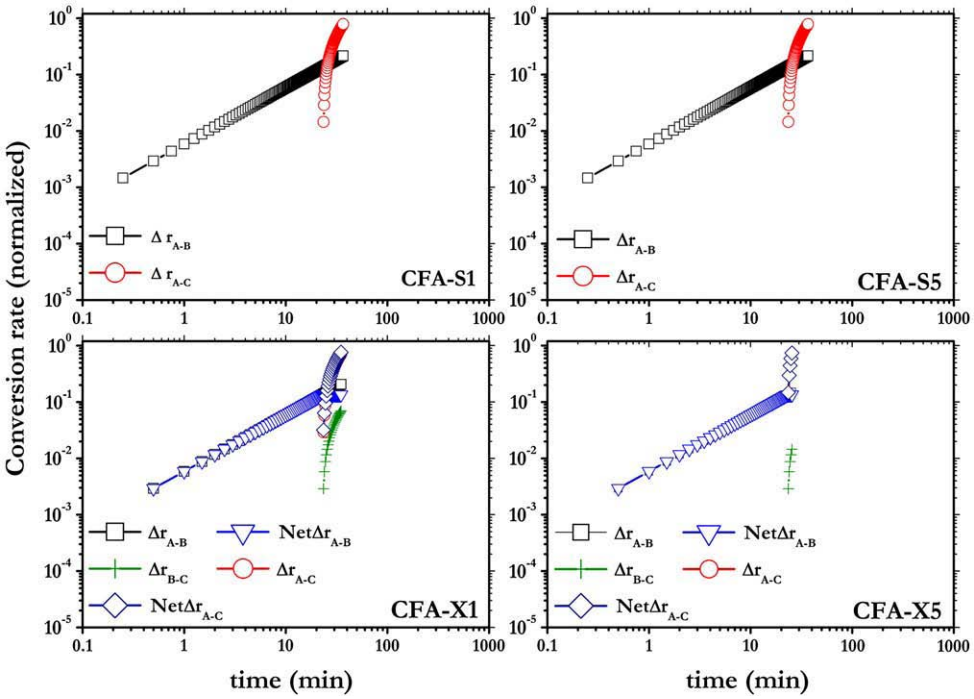

Fig. 3. Arrhenius simulation of a CFA processing: upper graphs stand for the simple model and bottom graphs for the complex model.

reported data. Part of the system reaches the **C** state directly from A, due to the fact that the system has enough potential energy to do so, but another part reaches first the fluorite phase (**B**) and then, after higher temperatures, evolves to the perovskite phase **C**.

4. Influence of the energy of activation of the process A–B on the overall behaviour of the system

The results obtained in the previous section were calculated assuming that the activation energy for the process **A→B** is around 164 kJ/mol. Two similar simulation runs were made by setting two different energies for the process **A→B**, i.e. the transformation from a initial reactive phase into the fluorite phase. Table 2 summarizes the final conversion values for each species, obtained for the same simulation process but using two different values of the activation energies for the **A→B** process. In this case the values were 110 and 200 kJ/mol, which are 50 kJ/mol below and above the value assumed initially.

Although not coincident, the results obtained in both sets of simulations are not significantly different from the previous ones. The observed similarities of the final results for processes having different activation energies for the initial step are somewhat expected, because from the very beginning it was assumed that the formation of the perovskite phase is favoured.

Table 2
Simulations results of the conversion of A into B or C by using two distinct activation energies for the process **A–B** (only the reactions **A→B** and **A→C** are shown).

	$E_{A-B}=110$ kJ/mol		$E_{A-B}=200$ kJ/mol	
	A→B	A→C	A→B	A→C
RTA-S1	0.0917	0.8984	0.0908	0.8992
RTA-S5	0.0199	0.9706	0.0197	0.9708
RTA-X1	0.0018	0.9883	8.52E−4	0.9891
RTA-X5	5.12E−4	0.9901	2.91E−4	0.9901
CFA-S1	0.2477	0.7425	0.2450	0.7464
CFA-S5	0.1671	0.8306	0.1650	0.8306
CFA-X1	0.1478	0.8423	0.1489	0.8472
CFA-X5	0.1505	0.8472	0.1484	0.8472

5. Conclusions

As previously stated, based on experimental results several authors have suspected that different reaction mechanisms occur depending of the rate of heating used in CFA or RTA processing. Oppositely, the results here presented and the analysis of reported data suggest a different scenario.

From the here described numerical simulations it is concluded that RTA and CFA are heating procedures implying reaction mechanisms chemically equivalent. Two different pathways (**A→B→C** and **A→C**) are predicted here to be present in fast and slow heating procedures. However, the heating rate favours the extension of one of these reactions mechanism over the other (**A→B→C** in the CFA treatment and **A→C** in RTA) , possibly because the transition state for the reaction **initial reactive phase→fluorite** is very similar (geometrically speaking) to the transition state of the reaction **initial reactive phase→Aurivillius (perovskite)**. The fast temperature (and energy) increase in the RTA process makes easy to pass from a transition state to the other, without passing by the local energy minimum represented by the fluorite phase. The observed experimental differences in the quality (or electro-opto-mechanical properties) of the materials prepared by these RTA or CFA are possibly originated by chemical contamination of the samples by small quantities of second phases (possibly fluorite).

An additional reasoning may now complete the previous conclusions: as the grain growth in the final material starts after the nucleation of the Aurivillius phase [17], and the reaction in RTA is several times faster than in CFA, different grain sizes for RTA or CFA processed samples are foreseen provided the rest of the experimental conditions are maintained unaltered [3].

Finally, the Arrhenius equation was never used in the differentiation of the mechanisms taking part in a complex reaction scheme in the solid state science. The results here presented confirm the validity of such equation in dealing with the complexity of the phenomena occurring in solid state reactions.

References

[1] K. Amanuma, T. Hase, Y. Miyasaka, Appl. Phys. Lett. 66 (1995) 221.
[2] I. Koiwa, T. Kanehara, J. Mita, T. Iwabuchi, T. Osaka, S. Ono, M. Maeda, Jpn. J. Appl. Phys. 35 (1996) 4946.

[3] I. Koiwa, K. Tani, T. Iwabuchi, Jpn. J. Appl. Phys. 137 (1998) 192.
[4] R. Jiménez, C. Alemany, M.L. Calzada, P. Tejedor, J. Mendiola, J. Eur. Ceram. Soc. 21 (2001) 1601.
[5] E.K.F. Dang, R.J. Gooding, Phys. Rev. Lett. 74 (1995) 3848.
[6] E.K.F. Dang, R.J. Gooding, Phys. Rev., E 54 (1996) 1383.
[7] G.D. Hu, X. Wilson, J.B. Xu, W.Y. Cheung, N. Ke, S.P. Wong, H.K. Wong, Appl. Phys. Lett. 74 (1999) 1221.
[8] W.-Ch. Kwak, Y.-M. Sung, J. Eur. Ceram. Soc. 24 (2004) 1603.
[9] W.-Ch. Kwak, Y.-M. Sung, J. Mater. Res. 17 (2002) 1463.
[10] M.L. Calzada, A. González, J. García-López, R. Jiménez, Chem. Mater. 15 (2003) 4775.
[11] R. Jiménez, C. Alemany, M.L. Calzada, A. González, J. Ricote, J. Mendiola, Appl. Phys., A 75 (2002) 607.
[12] M. Mortimer, Chemical Kinetics and Mechanisms, Royal Society of Chemistry, London, 2002.
[13] Y.-M. Sung, W.-Ch. Kwak, Chem. Phys. Lett. 411 (2005) 389.
[14] Z.-C. Wang, S. Mei, S. Karato, R. Wirth, Phys. Chem. Miner. 27 (1999) 11.
[15] K. Saito, M. Mitsuya, N. Nukaga, I. Yamaji, T. Akai, H. Funakubo, Jpn. J. Appl. Phys. 39 (2000) 5489.
[16] Y.-M. Sung, G.M. Anilkumar, S.-J. Hwang, J. Mater. Res. 18 (2003) 387.
[17] D.Ch. Yoo, J.Y. Lee, I.S. Kim, Y.T. Kim, J. Cryst. Growth 259 (2003) 79.
[18] M.L. Calzada, A. González, R. Jiménez, C. Alemany, J. Mendiola, J. Eur. Ceram. Soc. 21 (2001) 1517.
[19] G. González-Aguilar, M.E.V. Costa, I.M. Miranda Salvado, J. Eur. Ceram. Soc. 25 (2005) 2331.
[20] G. González-Aguilar, A. Wu, M.A. Reis, A.R. Ramos, I.M. Miranda Salvado, E. Alves, M.E.V. Costa, Surf. Sci. 600 (2006) 1780.